Hindawi
International Journal of Optics
Volume 2019, Article ID 4270612, 10 pages
https://doi.org/10.1155/2019/4270612

Research Article

The Critical Adiabatic Linear Tapered Waveguide Combined with a Multimode Waveguide Coupler on an SOI Chip

C. L. Chiu and Yen-Hsun Liao

Department of Electronic Engineering, National Kaohsiung University of Science and Technology, No. 415 Jiangong Road, Kaohsiung 807, Taiwan

Correspondence should be addressed to C. L. Chiu; clchiu@nkust.edu.tw

Received 10 August 2019; Revised 12 October 2019; Accepted 17 October 2019; Published 11 November 2019

Guest Editor: Cheng-Mu Tsai

A multimode waveguide interference (MMI) coupler is combined with a critical linear tapered waveguide on a silicon-on-insulator (SOI) chip. When the TE_0 mode is a critical adiabatic mode conversion from a single-mode waveguide to an extreme linear tapered waveguide combined with an MMI, this linear tapered waveguide is achieved to the maximum divergence angle (i.e., the shortest length). The maximum divergence angle is expressed by $\theta \leq 2\tan^{-1}[(0.35W_{\mathrm{mmi}} - W_{\mathrm{s}})/(0.172L_{\mathrm{mmi}})]$ under a 1×1 MMI combined with this critical linear tapered waveguide. The expression formula is demonstrated by three different widths of a 1×1 MMI of $4\,\mu$m/$8\,\mu$m/$12\,\mu$m combined with the critical linear tapered waveguide. So, the maximum divergence angle is obtained at $\theta = 16^\circ/14^\circ/8^\circ$, with respect to this linear tapered waveguide loss of 0.022 dB/0.172 dB/0.158 dB, and this linear tapper length is reduced by 93.7%/92.9%/87.5% than the divergence angle $\theta = 1^\circ$. The output power of a 1×1 MMI combined with a critical linear tapered waveguide is enhanced at least 1.5 times under 0.95 above condition.

1. Introduction

In the last few years, there have been numerous advances in silicon photonics. Photonic devices on a silicon-on-insulator (SOI) chip with high-index contrast have high integration density. The main advantage of the optoelectronic component on an SOI structure is its good compatibilities [1]. Couplers and power dividers in photonic integrated circuits (PICs) are often implemented with multimode interference couplers (MMIs) for easy fabrication and broad bandwidth. The SOI platform is an area of interest in integrated optics at present and enables a size reduction of PICs. Therefore, their CMOS compatibility can provide optoelectronic integration on a chip in future applications [2]. MMIs are based on the expansion of a fundamental mode of the access waveguide into multiple modes of the wider width of a multimode waveguide, which interfere as they propagate and form images of the excitation. Ridge waveguides are widely used in SOI, as they offer a single-mode behaviour at micrometre scale [3]. MMIs depend on multimode waveguides, utilizing bends for higher order mode filtering. They generally propagate well, and the weak lateral confinement of narrow ridge waveguides makes it difficult to achieve high-performance devices [4].

In 2010, Thomson et al. proposed a method to achieve a reduction of optical loss through the use of linear tapers with input and output ports. The taper loss is reduced to below 1 dB without affecting static extinction [5]. In 2012, Sheng et al. proposed the compact and low-loss MMI coupler fabricated with CMOS technology. This tapered waveguide with a divergence angle θ of 1° combined with an MMI is fabricated on SOI with $0.13\,\mu$m CMOS technology to obtain an excess loss of only 0.06 dB [6]. Researchers have adopted the widest and longest linear tapered waveguide to be combined with an MMI coupler on an SOI chip in recent devices. This critical problem will increase manufacturing costs, so it is necessary to design an adiabatic tapered waveguide.

The losses inherent to a mode propagating waveguide must be reduced on the cross-sectional boundary between the single-mode waveguide and multimode waveguide. Because a tapered waveguide can change the spot size and

the shape of the optical mode to achieve high coupling efficiency in the cross section boundary [7], a tapered waveguide is necessary to achieve an adiabatic state [7–10]. That is, as the TE_0 mode from a single-mode waveguide is transmitted to the tapered waveguide, the other higher order TE modes are reduced to excited modes [11–17].

In this article, we propose an expression formula to design a terminal linear tapered waveguide to enhance the coupling efficiency output power of an MMI coupler to two times above. The low-loss and maximum divergence angle linear tapered waveguide combined with a 1×1 MMI on an SOI chip is achieved to an output power of above 0.95. The TE_0 mode component ratio is necessary to be above 97.85% in order to achieve a critical adiabatic mode conversion.

2. Device Structure

The cross section of an SOI structure is shown in Figure 1. The thickness of the upper cladding SiO_2 layer is 2 μm, and the Si layer is deposited at a height h_{co} of 220 nm on a 2 -μm-thick buried oxide layer based on a Si substrate. The refractive indices of Si and SiO_2 are $n_{Si} = 3.475$ and $n_{SiO2} = 1.444$, respectively. The ridge waveguide has a depth of 2.22 μm, and the effective core refractive index n_r of 2.509 and cladding refractive index n_c of 2.372 at an operating wavelength λ_0 of 1550 nm in a slab waveguide [18].

MMI couplers have higher tolerance to dimensional changes in the fabrication process, an easier fabrication process than other couplers, lower inherent loss, large optical bandwidth, and low polarization dependence [19]. Multimode waveguides excite numerous modes depending on their width and depth. The width of a fixed step index multimode waveguide W_{mmi} is generally referred to as $N \times M$ MMI coupler, where N and M indicate input and output ports. For high-index contrast waveguides, the penetration depth is very small so that $W_e \approx W_{mmi}$. However, the effective width W_e can correspond to the fundamental mode [18]:

$$W_e = W_{mmi} + \left(\frac{\lambda_0}{\pi}\right)\left(\frac{n_c}{n_r}\right)^{2\sigma}\left(n_r^2 - n_c^2\right)^{-1/2}, \quad (1)$$

where λ_0 is an operating wavelength and n_r and n_c are the effective core and cladding refractive indices, respectively. The term $\sigma = 0$ represents transverse electric (TE) mode and $\sigma = 1$ is for transverse magnetic (TM) mode. L_π is defined as the beat length of the two lowest order modes [19], as follows:

$$L_\pi = \frac{\pi}{\beta_0 - \beta_1} \cong \frac{4 n_r W_e^2}{3\lambda_0}, \quad (2)$$

where β_0 and β_1 are individual zero-order and first-order propagation constant. The term n_r is the effective core refractive index of the slab waveguide from which a 1×1 MMI coupler is made. W_e is the effective width of the MMI waveguide, and L_{mmi} is the exact imaging length [20]:

$$L_{mmi} = \frac{3}{4} L_\pi. \quad (3)$$

The geometric shape of a basic 1×1 MMI coupler is shown in Figure 2(a). A single-mode ridge waveguide with width W_s of 0.4 μm, length L_s of 100 μm, and a depth of 2.22 μm is calculated by the effective core refractive index n_r of 2.509 and the effective cladding refractive index n_c of 2.372 [17]. An MMI width adapted to 10/20/30 times the single waveguide of 0.4 um as an inspecting standard case. The widths of a 1×1 MMI W_{mmi} are choice of 4 μm/8 μm/12 μm respect to the beat lengths L_π of 45.7 μm/159.8 μm/342.9 μm from equation (2) at an operating wavelength of $\lambda_0 = 1550$ nm. Therefore, the exact image length of a 1×1 MMI L_{mmi} achieves 34.3 μm/119.8 μm/257.1 μm, respectively, by equation (3). A linear tapered waveguide combined with a 1×1 MMI is shown in Figure 2(b). The input/output port of this 1×1 MMI is a single-mode waveguide linked with a linear tapered waveguide. W_t is the width and L_t the length of a linear tapered waveguide. The divergence angle θ of a linear tapered waveguide is a taper angle. A half angle of the divergence angle is defined by the following equation:

$$\tan\left(\frac{\theta}{2}\right) = \frac{W_t - W_s}{2L_t}. \quad (4)$$

The simulation analysis utilizes the film mode matching method (FMM) solver in FIMMWAVE software [21,22]. The output power of a basic 1×1 MMI with the exact length L_{mmi} is shown in Figure 3. Figure 3(a) is the length L_{mmi} of a 1×1 MMI scanning the range from 26.7 μm to 30.7 μm with a step of 0.2 μm at MMI width $W_{mmi} = 4$ μm. The maximum output power is 0.62 at $L_{mmi} = 28.7$ μm. Figure 3(b) is the length L_{mmi} of a 1×1 MMI scanning the range from 111.0 μm to 115.0 μm with a step of 0.2 μm at MMI width $W_{mmi} = 8$ μm. Here, the maximum output power is 0.51 at $L_{mmi} = 113.0$ μm. Figure 3(c) is the same method at MMI width $W_{mmi} = 12$ μm for L_{mmi} scanning the range from 255.2 μm to 259.2 μm. Maximum output power is 0.41 at $L_{mmi} = 257.2$ μm. Accordingly, L_{mmi} at MMI width $W_{mmi} = 4$ μm/8 μm/12 μm is 28.7 μm/113.0 μm/257.2 μm, respectively. The device loss of a 1×1 MMI is 2.08 dB/2.92 dB/3.87 dB, respectively, which is very significant.

3. Linear Tapered Waveguide Analysis

When the divergence angle of a linear tapered waveguide is set at $\theta = 1^\circ$ with a width W_t of 4.2 μm and a length L_t of 217.7 μm as an experimental standard result from reference 6, this pair of tapered waveguide loss of almost 0.004 (0.018 dB) can be ignored. This linear tapered waveguide with a divergence angle of 1° is combined with the three different widths of 1×1 MMI W_{mmi} of 4 μm/8 μm/12 μm with respect to the exact imaging lengths L_{mmi} of 28.7 μm/113.0 μm/257.2 μm. When the ratio of W_t/W_{mmi} is increased from 0.1 to 1 at a step of 0.05, the range of the output power increases from 0.68 to 1, as shown in Figure 4. The output power of a 1×1 MMI combined with the linear tapered waveguide is necessary to be above 0.95 as the ratio of W_t/W_{mmi} is set to above 0.35.

Figure 5 shows the effective refractive index n_{eff} for eight TE eigenmodes, including TE_0, TE_1, TE_2, TE_3, TE_4, TE_5, TE_6, and TE_7 distributed with the width of a linear tapered

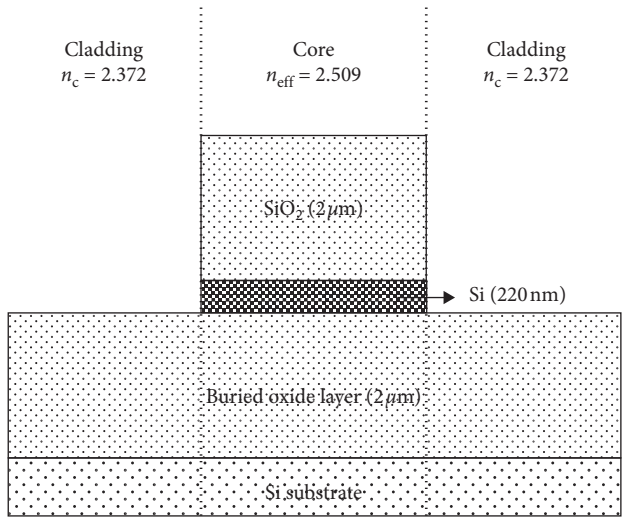

Figure 1: Schematic diagram showing the cross section of a ridge waveguide on an SOI structure.

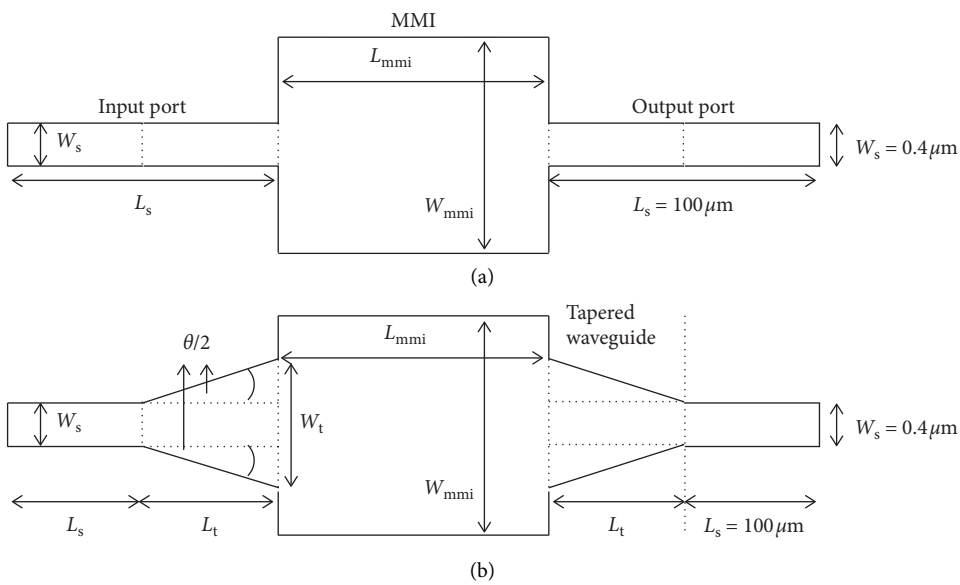

Figure 2: (a) A basic 1×1 MMI combined with the input/output single-mode waveguide for width $W_s = 0.4\,\mu$m and length $L_s = 100\,\mu$m. (b) A linear tapered waveguide is inserted between the single-mode waveguide and MMI coupler. Width W_t, length L_t, and divergence angle θ describe the linear tapered waveguide.

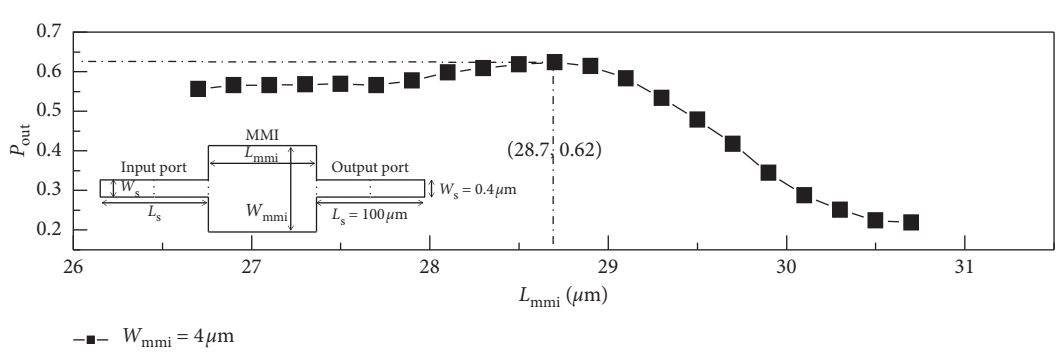

(a)

Figure 3: Continued.

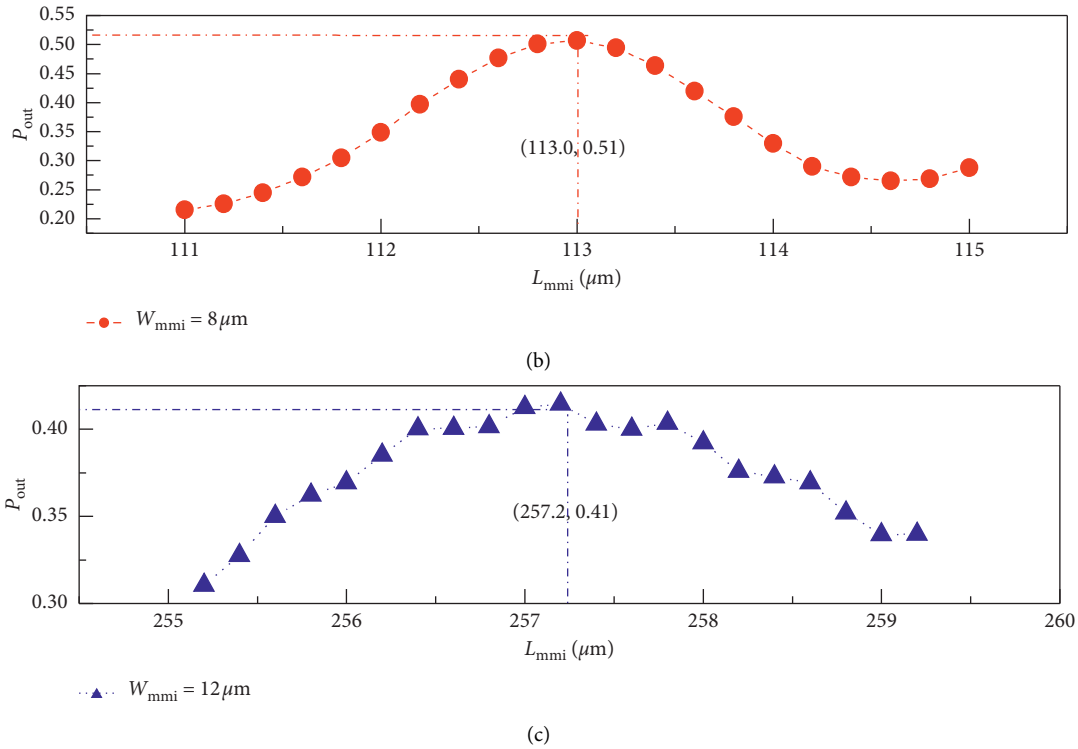

Figure 3: (a) The maximum output power is 0.62 at MMI length $L_{mmi} = 28.7\,\mu$m with a 1×1 MMI width $W_{mmi} = 4\,\mu$m. (b) Maximum output power is 0.51 at $L_{mmi} = 113.0\,\mu$m and $W_{mmi} = 8\,\mu$m. (c) Maximum output power is 0.41 at $L_{mmi} = 257.2\,\mu$m and $W_{mmi} = 12\,\mu$m.

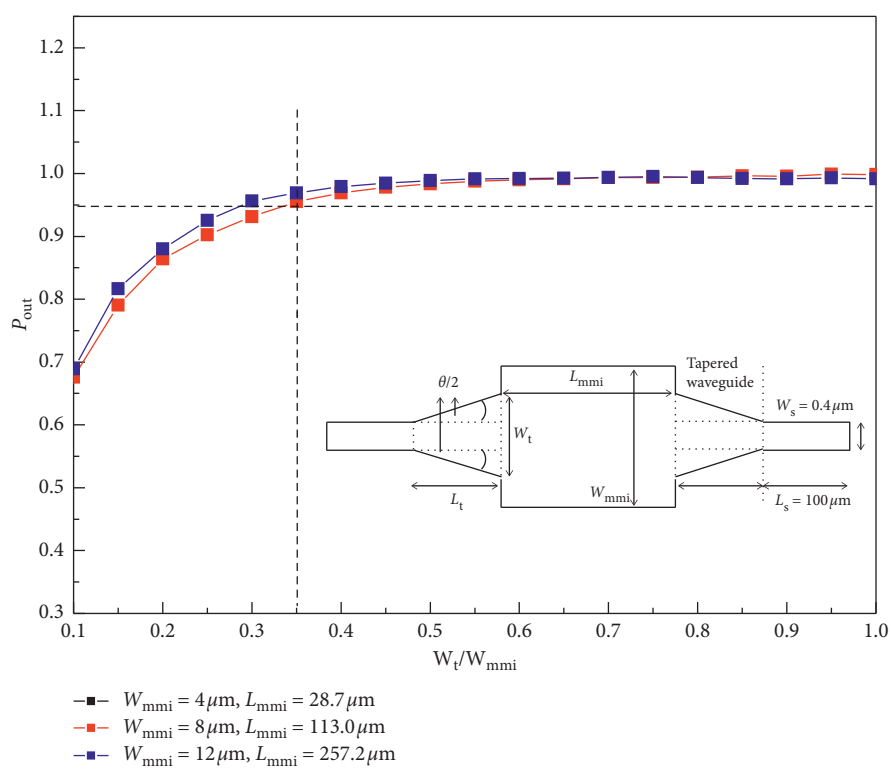

Figure 4: This linear tapered waveguide with a divergence angle of 1° is combined with the three different widths of a 1×1 MMI coupler W_{mmi} of $4\,\mu$m/$8\,\mu$m/$12\,\mu$m with respect to the exact imaging lengths L_{mmi} of $28.7\,\mu$m/$113.0\,\mu$m/$257.2\,\mu$m. When W_t/W_{mmi} is set at above 0.35, the output power P_{out} of a 1×1 MMI coupler combined with a linear tapered waveguide achieves above 0.95.

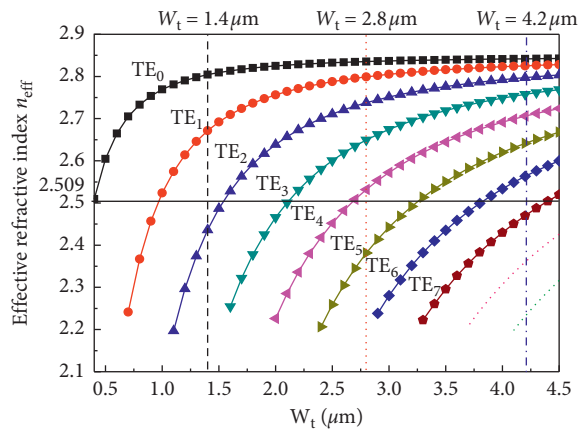

Figure 5: The effective refractive index of the distributed state of eight TE modes with the width of a linear tapered waveguide is ranging from 0.4 μm to 4.5 μm. The effective refractive index n_{eff} of the slab waveguide on an SOI chip is 2.509 and the thickness of this linear tapered waveguide h_{co} is 220 nm at an operating wavelength of 1550 nm.

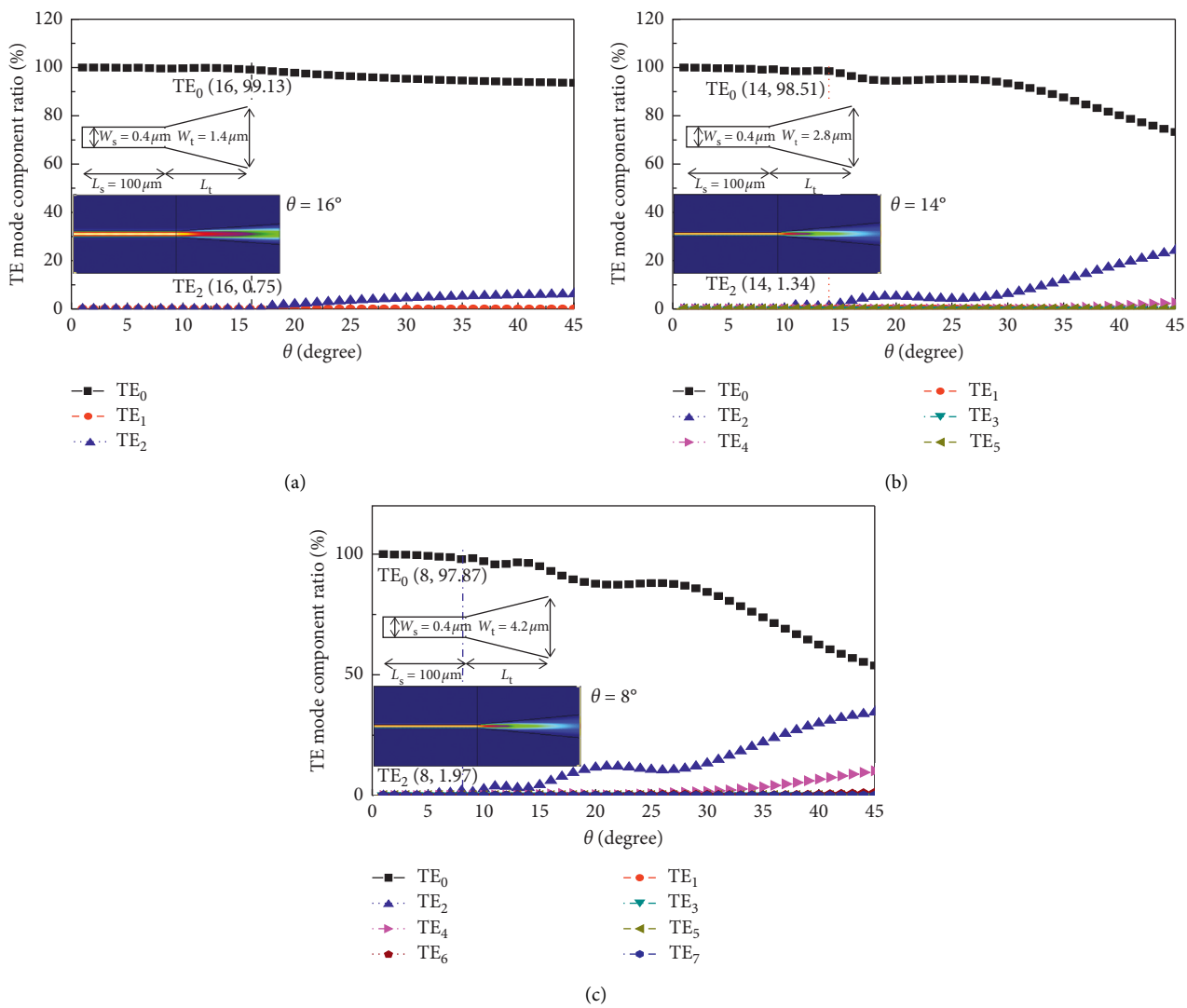

Figure 6: The width of a linear tapered waveguide (a) $W_t = 1.4\,\mu m$, $W_{mmi} = 4\,\mu m$; (b) $W_t = 2.8\,\mu m$, $W_{mmi} = 8\,\mu m$; (c) $W_t = 4.2\,\mu m$, $W_{mmi} = 12\,\mu m$; with divergence angle θ of a linear tapered waveguide ranging from 1° to 45°. The maximum divergence angle for linear tapered waveguide is achieved at $\theta = 16°/14°/8°$ for $W_t = 1.4\,\mu m/2.8\,\mu m/4.2\,\mu m$, respectively.

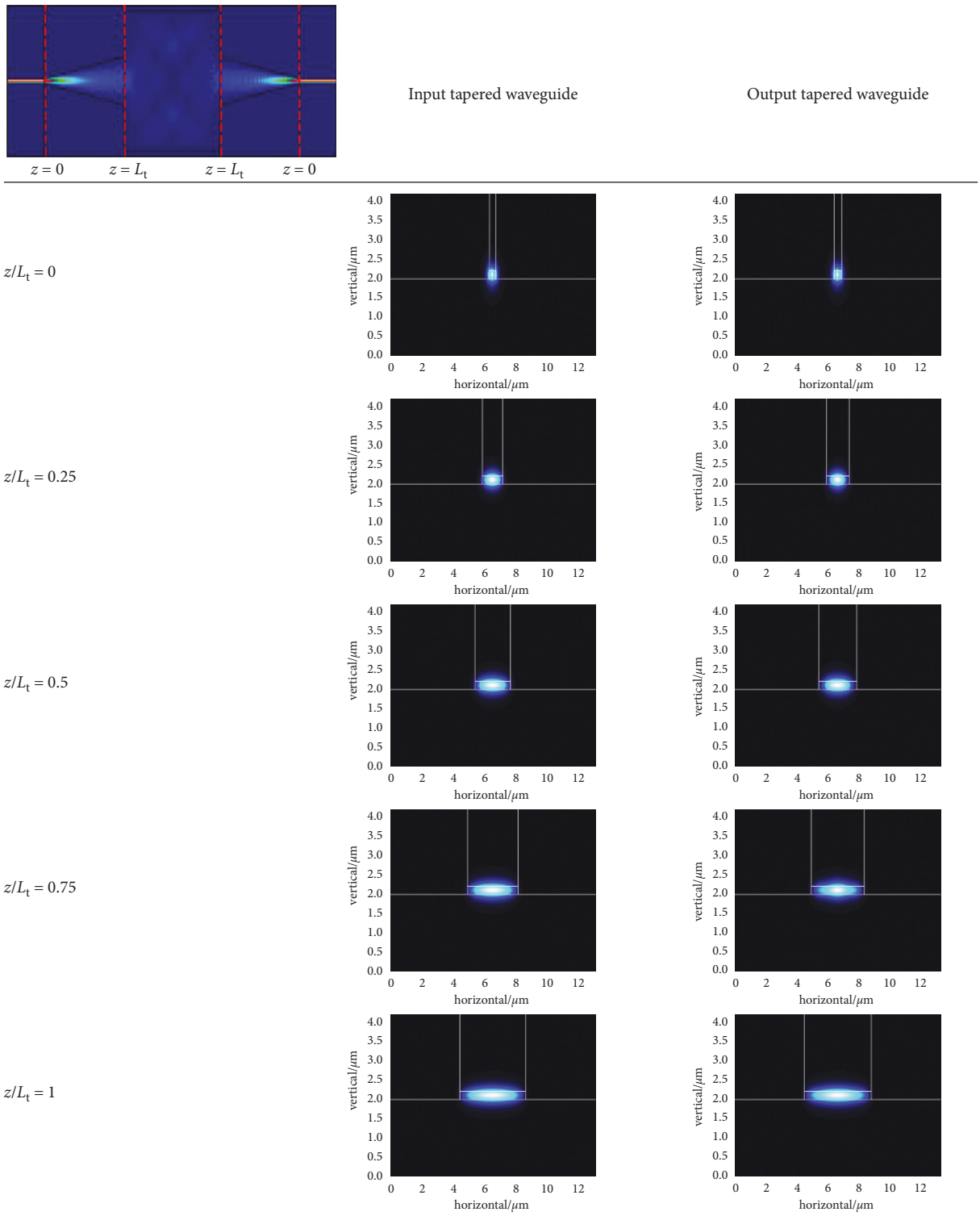

Figure 7: A 1×1 MMI in width of 12 μm and in length of 257.2 μm is combined with the linear tapered waveguide in width W_t of 4.2 μm and in length L_t of 217.7 μm. When the location of input/output linear tapered waveguide is z/L_t of 0/0.25/0.5/0.75/1, the fundamental mode TE_0 shape of input/output port is simulated to change the mode shape size from small to larger mode shape under TE_0 adiabatic mode conversion.

waveguide from 0.4 μm to 4.5 μm. As the effective refractive index n_{eff} of a slab waveguide on an SOI chip is 2.509, the eight TE eigenmodes, including TE_0 to TE_7, correspond to the widths of the linear tapered waveguide W_t. Three different widths of 1×1 MMI W_{mmi} of 4 μm/8 μm/12 μm obtain a minimum width for a linear tapered waveguide W_t of 1.4 μm/

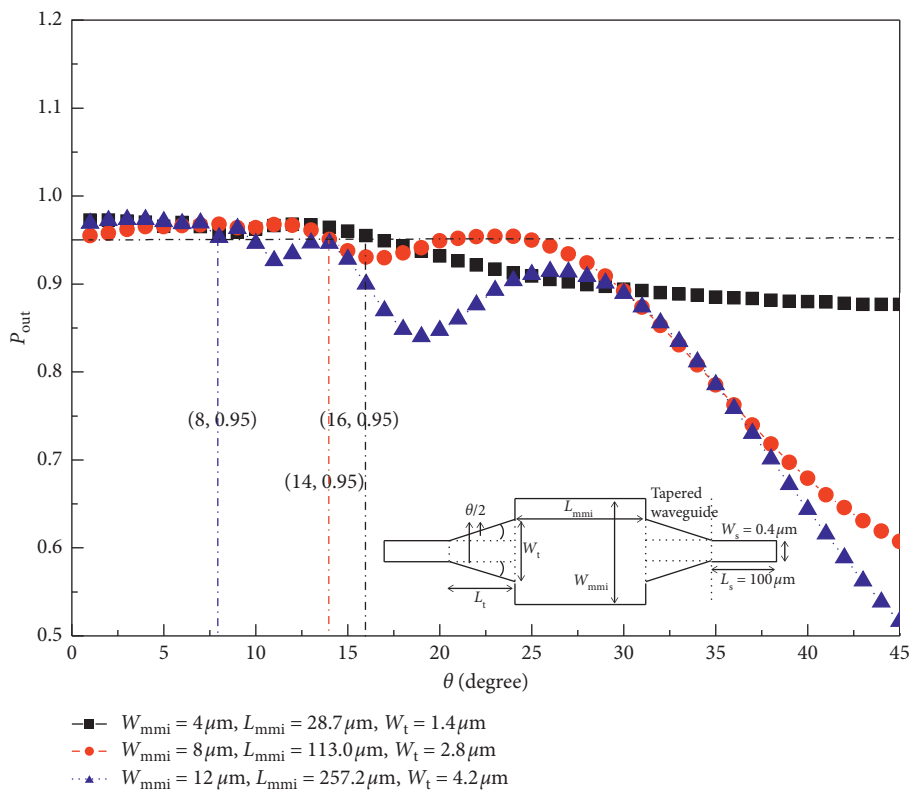

FIGURE 8: When W_t/W_{mmi} is set at 0.35, the 1×1 MMI coupler with $W_{mmi} = 4\,\mu m/8\,\mu m/12\,\mu m$ achieves a minimum width of linear tapered waveguide at $W_t = 1.4\,\mu m/2.8\,\mu m/4.2\,\mu m$, respectively. As the divergence angle θ of a linear tapered waveguide is scanning the range from 1° to 45° at a step of 1°, a maximum divergence angle $\theta = 16°/14°/8°$ is obtained under the constraint of $P_{out} \geq 0.95$, respectively.

$2.8\,\mu m/4.2\,\mu m$, respectively. As the TE_0 mode is transmitted from a single-mode waveguide with a width of $0.4\,\mu m$ into a linear tapered waveguide with a width W_t of $1.4\,\mu m$, TE_0 and TE_1 are excited. The taper width W_t of $2.8\,\mu m$ is excited for TE_0, TE_1, TE_2, TE_3, and TE_4 modes. The taper width W_t of $4.2\,\mu m$ is excited for TE_0, TE_1, TE_2, TE_3, TE_4, TE_5, and TE_6 modes. As the geometric shape of the device is symmetrical structure, the odd modes are suppressed and inexistent.

The single-mode waveguide with width W_s of $0.4\,\mu m$ is combined with the width of the linear tapered waveguide W_t of $1.4\,\mu m/2.8\,\mu m/4.2\,\mu m$, respectively. TE mode component ratio is distributed with the divergence angle of a linear tapered waveguide ranging from 1° to 45°, as shown in Figure 6. When the even modes of TE_2, TE_4, and TE_6 and the odd modes of TE_1, TE_3, TE_5, and TE_7 except TE_0 are suppressed in the linear tapered waveguide, the maximum divergence angle θ of the linear tapered waveguide is 16°/14°/8° with respect to a 1×1 MMI with width W_{mmi} of $4\,\mu m/8\,\mu m/12\,\mu m$. The TE_0 mode component ratio obtains individual 99.13%/98.51%/97.87%. So, this linear tapered waveguide achieves the TE_0 mode adiabatic mode conversion when the TE_0 mode component ratio is at least 97.87% and TE_2 mode and the other modes component ratio is below 2.13%.

For a standard adiabatic mode conversion analysis, a 1×1 MMI in width of $12\,\mu m$ and in length of $257.2\,\mu m$ is combined with the divergence angle $\theta = 1°$ of linear tapered waveguide in width W_t of $4.2\,\mu m$ and in length L_t of $217.7\,\mu m$. When the location of input/output linear tapered waveguide is z/L_t of 0/0.25/0.5/0.75/1, the fundamental mode TE_0 shape of input/output port is simulated to change the mode shape size from smaller to larger mode shape under TE_0 adiabatic mode conversion as shown in Figure 7. The coupling efficiency of this device between the single-mode waveguide and the multimode waveguide is enhanced from 0.41 to 0.95.

The 1×1 MMI with width W_{mmi} of $4\,\mu m/8\,\mu m/12\,\mu m$ is combined with the width of the linear tapered waveguide W_t of $1.4\,\mu m/2.8\,\mu m/4.2\,\mu m$, respectively, as the input and output port with the divergence angle θ of a linear tapered waveguide scanning the range from 1° to 45° at a step of 1°. The maximum divergence angle θ is achieved at 16°/14°/8°, respectively, under the condition of output power of a 1×1 MMI combined with a linear tapered waveguide of at least 0.95, as shown in Figure 8. Figure 9 shows that the spectral responses are insensitivity for the wavelength from 1546 to 1554 nm with the step of 1 nm under the condition of this linear tapered waveguide with a maximum divergence angle θ of 16°/14°/8° combined with the three different widths of a 1×1 MMI of $4\,\mu m/8\,\mu m/12\,\mu m$, respectively. The output power of three different widths of a 1×1 MMI linked with the maximum divergence angle θ of 16°/14°/8° of a linear tapered waveguide is 0.95 when the ratio of W_t/W_{mmi} is equal to 0.35. Three different divergence angles θ of the linear tapered waveguide of 16°/14°/8° with respect to three different widths of a 1×1 MMI width W_{mmi} of $4\,\mu m/8\,\mu m/12\,\mu m$ are taken into equation (4).

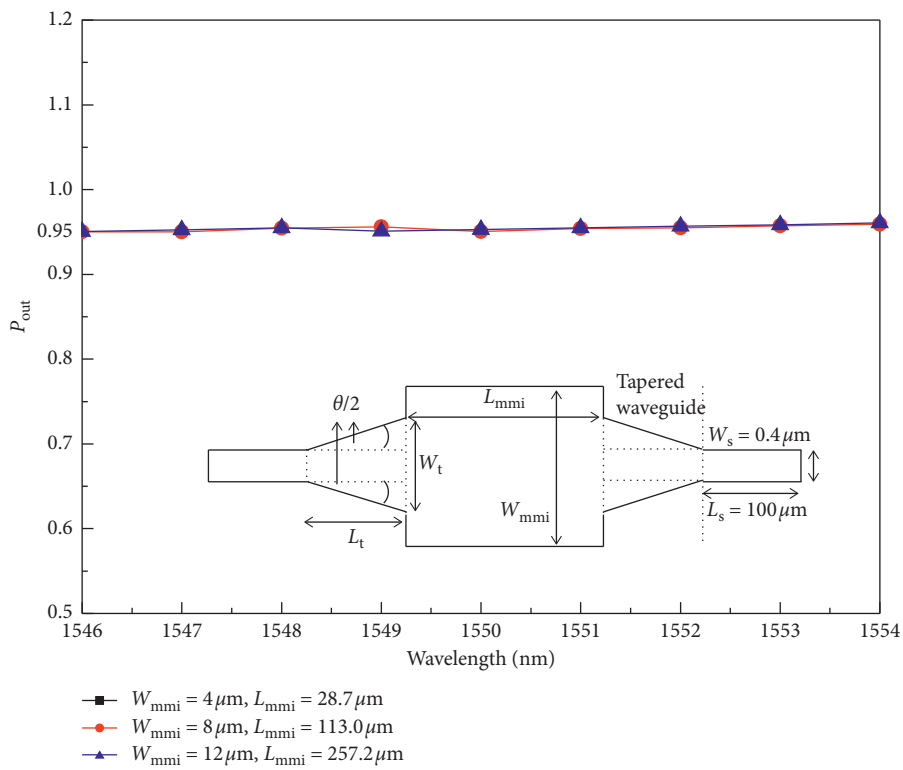

Figure 9: The spectral responses are insensitivity for the wavelength from 1546 to 1554 nm with the step of 1 nm under the condition of this linear tapered waveguide with a maximum divergence angle θ of 16°/14°/8° combined with the three different widths of a 1×1 MMI of 4 μm/8 μm/12 μm, respectively.

Table 1: A basic 1×1 MMI device loss.

W_{mmi} (μm)	L_{mmi} (μm)	Pout (device loss (dB))
4	28.7	0.62(2.08 dB)
8	113.0	0.51(2.92 dB)
12	257.2	0.41(3.87 dB)

The length of a linear tapered waveguide L_t is calculated by 3.6 μm/9.8 μm/27.2 μm, respectively. The ratio of the length of a linear tapered waveguide to the length of a 1×1 MMI is expressed as $L_t/L_{mmi} \geqq 0.086$.

The expressions of equations (5) and (6) are demonstrated under three different widths of a 1×1 MMI coupler combined with a designed linear tapered waveguide:

$$W_t \geq 0.35 W_{mmi}, \tag{5}$$

$$L_t \geq 0.086 L_{mmi}, \tag{6}$$

where W_t is the width of the linear tapered waveguide, L_t is the length of the linear tapered waveguide, and W_{mmi} is the width of a 1×1 MMI and L_{mmi} of the exact imaging length of a 1×1 MMI. When the width of the single-mode waveguide W_s of 0.4 μm and equations (5) and (6) are taken into equation (4), the maximum divergence angle, θ, is expressed as equation (7).

$$\theta \leq 2 \tan^{-1}\left(\frac{0.35 W_{mmi} - W_s}{0.172 L_{mmi}}\right). \tag{7}$$

Comparison of basic 1×1 MMI device loss with a 1×1 MMI combined with a linear tapered waveguide device loss is shown in Tables 1 and 2. When 1×1 MMI with width W_{mmi} of 4 μm/8 μm/12 μm is combined with a maximum divergence angle $\theta = 16°/14°/8°$ in a linear tapered waveguide with a width W_t of 1.4 μm/2.8 μm/4.2 μm and length L_t of 3.6 μm/9.8 μm/27.2 μm, the loss of this linear tapered waveguide is 0.022 dB/0.172 dB/0.158 dB. The length of a maximum divergence angle $\theta = 16°/14°/8°$ in this linear tapered waveguide is reduced to 93.7%/92.9%/87.5% than the length of the divergence angle $\theta = 1°$ combined a 1×1 MMI with width of 4 μm/8 μm/12 μm. The output power of a 1×1 MMI combined with the maximum divergence angle of a linear tapered waveguide is 0.95 (0.22 dB). A 1×1 MMI device loss with a linear tapered waveguide reduces 1.86 dB/2.70 dB/3.65 dB than a 1×1 MMI device loss without a linear

Table 2: A 1×1 MMI combined with a linear tapered waveguide device loss.

Pout (Device loss (dB))	W_t (μm)	Max. divergence angle (degree)	Linear tapered waveguide loss (dB)
0.95 (0.22 dB)	1.4	16°	0.022
0.95 (0.22 dB)	2.8	14°	0.172
0.95 (0.22 dB)	4.2	8°	0.158

tapered waveguide. This device loss represents a significant reduction.

4. Conclusion

A 1×1 MMI is combined with a symmetrical linear tapered waveguide on an SOI chip. When TE_0 mode from a single-mode waveguide is transmitted to this critical linear tapered waveguide linked with a 1×1 MMI, the TE_0 mode component ratio is necessary to be at least 97.87% and the TE_2 mode and the other modes' component ratios are to be below 2.13%. So, the TE_0 mode presents a critical adiabatic mode conversion. The designed linear tapered waveguide is achieved to the shortest length and the maximum divergence angle.

Under the condition of a 1×1 MMI coupler combined with the designed linear tapered waveguide, the maximum divergence angle is demonstrated by $\theta \leq 2 \tan^{-1} [(0.35 W_{mmi} - W_s)/(0.172 L_{mmi})]$. When the width of a 1×1 MMI W_{mmi} is 4 μm/8 μm/12 μm with respect to the length L_{mmi} of 28.7 μm/113.0 μm/257.2 μm, the maximum divergence angle θ is achieved to 16°/14°/8°, respectively.

A 1×1 MMI width W_{mmi} of 4 μm/8 μm/12 μm combined with a maximum divergence angle $\theta = 16°/14°/8°$ linear tapered waveguide to a 1×1 MMI without linear tapered waveguide. The simulation result shows that the device loss is reduced by 1.86 dB/2.70 dB/3.65 dB, respectively, with respect to an extreme linear tapered waveguide loss of 0.022 dB/0.172 dB/0.158 dB. The length of a maximum divergence angle $\theta = 16°/14°/8°$ linear tapered waveguide is reduced to 93.7%/92.9%/87.5% than the length of the divergence angle $\theta = 1°$ linear tapered waveguide combined with a 1×1 MMI with width of 4 μm/8 μm/12 μm. The output power of a 1×1 MMI combined with a critical linear tapered waveguide is at least 0.95, which enhanced the coupling efficiency by 1.5 times.

Data Availability

The data used to support the findings of this study are included within the article files.

Conflicts of Interest

The authors declare that they have no conflicts of interest.

Acknowledgments

This work was supported in part by the Ministry of Science and Technology, Taiwan, Republic of China, under the grant no. MOST 108-2221-E-992-080.

References

[1] R. Soref, "The past, present, and future of silicon photonics," *IEEE Journal of Selected Topics in Quantum Electronics*, vol. 12, no. 6, pp. 1678–1687, 2006.

[2] M. Lipson, "Guiding, modulating, and emitting light on silicon-challenges and opportunities," *Journal of Lightwave Technology*, vol. 23, no. 12, pp. 4222–4238, 2005.

[3] K. Kruse and C. T. Middlebrook, "Polymer taper bridge for silicon waveguide to single mode waveguide coupling," *Optics Communications*, vol. 362, pp. 87–95, 2016.

[4] J. Guo and Y. Zhao, "Analysis of mode hybridization in tapered waveguides," *IEEE Photonics Technology Letters*, vol. 27, no. 23, pp. 2441–2444, 2015.

[5] D. J. Thomson, Y. Hu, G. T. Reed, and J.-M. Fedeli, "Low loss MMI couplers for high performance MZI modulators," *IEEE Photonics Technology Letters*, vol. 22, no. 20, pp. 1485–1487, 2010.

[6] Z. Sheng, Z. Zhiqi Wang, C. Chao Qiu et al., "A compact and low-loss MMI coupler fabricated with CMOS technology," *IEEE Photonics Journal*, vol. 4, no. 6, pp. 2272–2277, 2012.

[7] P. Sethi, A. Haldar, and S. K. Selvaraja, "Ultra-compact low-loss broadband waveguide taper in silicon-on-insulator," *Optics Express*, vol. 25, no. 9, pp. 10196–10203, 2017.

[8] Y. Liu, W. Sun, H. Xie et al., "Adiabatic and ultra-compact waveguide tapers based on digital metamaterials," *IEEE Journal of Selected Topics in Quantum Electronics*, vol. 25, no. 3, pp. 1–6, 2018.

[9] J. Zhang, J. Yang, H. Xin, J. Huang, D. Chen, and Z. Zhaojian, "Ultrashort and efficient adiabatic waveguide taper based on thin flat focusing lenses," *Optics Express*, vol. 25, no. 17, pp. 19894–19903, 2017.

[10] Y. Fu, T. Ye, W. Tang, and T. Chu, "Efficient adiabatic silicon-on-insulator waveguide taper," *Photonics Research*, vol. 2, no. 3, pp. A41–A44, 2014.

[11] J. Wang, M. Qi, Y. Xuan et al., "Proposal for fabrication-tolerant SOI polarization splitter-rotator based on cascaded MMI couplers and an assisted bi-level taper," *Optics Express*, vol. 22, no. 23, pp. 27869–27879, 2014.

[12] Y. Zhang, S. Yang, A. E.-J. Lim et al., "A CMOS-compatible, low-loss, and low-crosstalk silicon waveguide crossing," *IEEE Photonics Technology Letters*, vol. 25, no. 5, pp. 422–425, 2013.

[13] D. Dai, Y. Tang, and J. E. Bowers, "Mode conversion in tapered submicron silicon ridge optical waveguides," *Optics Express*, vol. 20, no. 12, pp. 13425–13439, 2012.

[14] L. He, Y. He, A. Pomerene et al., "Ultrathin silicon-on-insulator grating couplers," *IEEE Photonics Technology Letters*, vol. 24, no. 24, pp. 2247–2249, 2012.

[15] C.-H. Chen and C.-H. Chiu, "Taper-integrated multimode-interference based waveguide crossing design," *IEEE Journal of Quantum Electronics*, vol. 46, no. 11, pp. 1656–1661, 2010.

[16] W. Bogaerts, P. Dumon, D. V. Thourhout, and R. Baets, "Low-loss, low-cross-talk crossings for silicon-on-insulator nano-photonic waveguides," *Optics Letters*, vol. 32, no. 19, pp. 2801–2803, 2007.

[17] J. J. Wu, B. R. Shi, and M. Kong, "Exponentially tapered multimode interference couplers," *Chinese Optics Letters*, vol. 4, no. 3, pp. 167–169, 2006.
[18] P. K. Bhattacharya, *Semiconductor Optoelectronic Devices*, Prentice-Hall, Englewood Cliffs, NJ, USA, 1998.
[19] L. B. Soldano and E. C. M. Pennings, "Optical multi-mode interference devices based on self-imaging: principles and applications," *Journal of Lightwave Technology*, vol. 13, no. 4, pp. 615–627, 1995.
[20] M. Bachmann, P. A. Besse, and H. Melchior, "Overlapping-image multimode interference couplers with a reduced number of self-images for uniform and nonuniform power splitting," *Applied Optics*, vol. 34, no. 30, pp. 6898–6910, 1995.
[21] A. S. Sudbo, "Film mode matching: a versatile numerical method for vector mode field calculations in dielectric waveguides," *Pure and Applied Optics: Journal of the European Optical Society Part A*, vol. 2, no. 3, pp. 211–233, 1993.
[22] *Integrated Optics Software FIMMWAVE 5.2*, Photon Design, Oxford, U.K, 2015, http://www.photond.com.